Environ. Sci. Technol. 1993, 27, 2360–2366

Desorption of Trichloroethylene in Aquifer Material: Rate Limitation at the Grain Scale

Peter Grathwohl[†] and Martin Reinhard*

Department of Civil Engineering, Environmental Engineering and Science, Stanford University, Stanford, California 94305-4020

Soil-gas venting for the removal of sorbed trichloroethylene (TCE) was studied in columns packed with either wet or oven-dry Santa Clara aquifer material. After the wet columns were vented up to 1 h, the removal rate was independent of the flow rate and limited by slow intraparticle mass transfer. In contrast, removal of TCE from columns filled with oven-dry material was proportional to the flow rate after 20 days of venting. This suggests that intraparticle pore water limits mass transfer from the internal sorption sites. Desorption was modeled using an intraparticle diffusion model assuming homogeneous porous spheres. The model was calibrated in batch sorption studies using the apparent diffusion rate constant as a fitting parameter.

Introduction

Detailed laboratory investigations have revealed that sorption and desorption of volatile organic compounds from aquifer materials, soils, and sediments occur over a broad range of time scales ranging from instantaneous to weeks and months (*1–8*). Understanding the mechanism of sorption and desorption is important for predicting fate and transport and for selecting cleanup technologies. One of the mechanistic models used to explain slow intraparticle mass transfer is the intraparticle diffusion model (*1–5*), which assumes that diffusion occurs in water-filled pores within homogeneous particles and that diffusion is retarded by equilibrium sorption within the pores. Other possible mechanistic models have been considered including slow diffusion in organic polymers such as humic substances and strong adsorption on internal surfaces (*3, 7, 9*). Experimental data obtained in the uptake mode do not unequivocally support one of the models, and conclusions about the sorption mechanisms and medium for solute diffusion remain tenuous (*4, 9*). In batch experiments, the approach to equilibrium is difficult to discern close to equilibration (within 1%) due to analytical limitations. Study of slow mass transfer is possible in the desorption mode by analyzing the desorbing mass with extremely sensitive chromatographic detectors (e.g., ref 9). The purpose of this study was to investigate sorption and desorption behavior of volatile organic compounds under soil-gas venting conditions using TCE and aquifer material from the Santa Clara Valley. Specific objectives were (i) to determine desorption rates from dry and moist solids to investigate the sorption mechanism and (ii) to evaluate the intraparticle diffusion model as a tool to predict cleanup times. Specific system parameters that were studied include water content, contaminant concentration, air flow rates, and preequilibration times. Only conditions below TCE saturation pressure were studied. Since the intraparticle diffusion model is invariant with respect to the direction of the diffusional mass flux, it should be possible to use sorption and desorption data to calibrate this model. At 99% relative humidity (RH), water covers the surfaces and fills the internal pore volume (up to pores with 100-nm radius), and therefore, sorption of hydrophobic compounds in the unsaturated system becomes comparable to sorption in a water-saturated system (*10, 11*). Thus, results of this study should also apply to transport under saturated conditions.

Theoretical Considerations

Mass balances were evaluated by assuming that TCE was either sorbed by solids (mineral or organic phases), dissolved in the soil water, or present as vapor (*10*). Henry's constant, H, indicates the distribution between the gas phase and the soil water and is independent of relative humidity above 95% (*12*). The soil/water distribution coefficient, K_d, is used to indicate equilibrium sorption in water-saturated systems. Combining both, we obtain

$$C_S = K_d C_W = K_d(C_G/H) \tag{1}$$

where C_S, C_W, and C_G denote the concentrations in solid, water, and vapor phases, respectively. Under nonequilibrium conditions, K_d is denoted as "apparent K_d" which is a function of time. The Freundlich equation is used to describe nonlinear isotherms (*13*): $C_S = K_{Fr}C_W^{1/n}$, where K_{Fr} and $1/n$ denote the Freundlich coefficient and exponent, respectively. For $1/n = 1$, $K_{Fr} = K_d$; for $1/n \neq 1$, the ratio C_S/C_W depends on the solute concentration.

The intraparticle diffusion model has been discussed in detail elsewhere (*1–4*). In this model, it is assumed that the particles are homogeneous spheres and that intraparticle transport can be described by a constant apparent diffusion coefficient, D_{app}. According to this model, the particle radius, a, is the appropriate length scale. In batch experiments using size fractions with a defined particle radius, D_{app} can be obtained by fitting experimental data on sorptive uptake to the appropriate analytical solution of Fick's second law in spherical coordinates using the diffusion rate constant, D_{app}/a^2, as a fitting parameter (*14*):

$$M_t/M_{eq} = 1 - \sum_{n=1}^{\infty} \frac{6\alpha(\alpha + 1)\exp(-q_n^2 t D_{app}/a^2)}{9 + 9\alpha + q_n^2\alpha^2} \tag{2}$$

where α is equal to the ratio of the mass of solute dissolved in the aqueous phase to the mass sorbed onto the solids in the batch experiment under equilibrium conditions. M_t and M_{eq} are the masses of the solute in the sphere at time t and at equilibrium, respectively. The q_n's denote the non-zero roots of $\tan q_n = 3q_n/(3 + \alpha q_n^2)$. The analytical expression of solute diffusing from a spherical soil particle, initially ($t = 0$) at sorption equilibrium, into bulk water

[†] Present address: Institute of Geology, Applied Geology Group, University of Tübingen, Ob dem Himmelreich 7, MNF, 72074 Tübingen, Germany.

0013-936X/93/0927-2360$04.00/0

or vapor kept solute-free for $t > 0$ is given by (*14*)

$$\frac{M_t}{M_0} = \frac{6}{\pi^2}\sum_{n=1}^{\infty}\frac{1}{n^2}\exp(-n^2\pi^2 t D_{app}/a^2) \quad (3)$$

where M_0 is the initial mass of solute in the sphere. The analytical solution for the desorption rate, q, is (15)

$$q = 6M_0\frac{D_{app}}{a^2}\sum_{n=1}^{\infty}\exp(-n^2\pi^2 t D_{app}/a^2) \quad (4)$$

If D_{app} is invariant with respect to the direction of diffusional transport, the D_{app}/a^2 factor determined in the sorptive uptake mode can be used to predict the desorption rate. The analytical solutions (eqs 3 and 4) have simple approximations for long and short desorption times. For long times ($tD_{app}/a^2 > 0.1$), only the first terms in eqs 3 and 4 are significant. Then M_t/M_0 or q vs t is linear on a log–linear plot with a slope of $-(\pi^2 D_{app}/a^2)$. On a log–log plot, the slope of M_t/M_0 vs t becomes progressively more negative. For short desorption times ($D_{app}/a^2 < 0.01$), q decreases linearly with the square root of time (*16*) and the slope of q vs t on a log–log plot is –0.5.

Assuming that (i) diffusion within the particle occurs in the aqueous phase, (ii) diffusion is retarded by equilibrium sorption within the pores, (iii) particles are homogeneous, and (iv) pores are of uniform diameter and much larger than the sorbate, D_{app} may be defined as follows:

$$D_{app} = \frac{D_{aq}\epsilon_i}{(\epsilon_i + K_d\rho)\tau_f} \quad (5)$$

where D_{aq} is the diffusion coefficient in bulk water, ρ_g is the bulk density of the grain, ϵ_i is the intraparticle porosity, and τ_f is the tortuosity factor. K_d, ρ_g, and ϵ_i of the solids can be determined experimentally as described below.

It is readily evident that for Freundlich isotherms with $1/n < 1$, the K_d increases with decreasing M_t, therefore q decreases slower with time than with linear sorption. However, for narrow concentration ranges as employed in the desorption experiments in this study, this effect was shown not to alter the desorption rates significantly (*8*, *16*).

Materials and Methods

Chemicals and Materials. All chemicals were obtained in the purest form available and used as received. The aqueous diffusion coefficient of TCE at 20 °C used was 8.4×10^{-6} cm²/s (*17*). The dimensionless Henry's coefficient (20 °C) used was 0.31 (*18*).

The sediment used was from an uncontaminated section of the Santa Clara Valley, CA. The material is late Pleistocene to recent, undeformed, and comprised of a wide variety of lithic fragments (*19*, *20*). Prevalent source rocks of the sediments are sandstones (chiefly graywacke) with shale intercalations; cherts and limestones in discontinuous lenses; and metamorphic, mafic, and volcanic rocks (*19*).

The aquifer material was first separated into a fraction larger than 1.98 mm and a fraction smaller than 1.98 mm by wet sieving. The fraction smaller than 1.98 mm consisted mainly of sand and is hereafter referred to as bulk sand (B). The fraction larger than 1.98 mm was separated by dry sieving into a fraction of 1.98–2.36-mm diameter subsequently referred to as sand—gravel (S). S was ultrasonicated in milli-Q water four times for approximately 3 min to remove clay coatings and dried overnight at 110 °C.

Table I. Mineralogical Composition and Properties of the Santa Clara Valley Aquifer Material and Results of Batch Sorption Experiments

sample	B	S
Composition		
quartz, chert (%)	29.7	17.7
igneous–metamorphic rock fragments (%)	16.1	21.5
fragments of sedimentary rocks		
sandstone, gravywacke (%)	40.9	41.5
shale (%)	13.3	19.2
Properties		
specific surface area (m²/g)	13.2	12.6
intraparticle porosity ϵ_i	0.049	0.026
nominal radius (cm)[a]	0.025	0.108
Freundlich Isotherms		
K_{Fr} (L/kg)	3.5	4.3
$1/n$	0.56	0.62
Long-Term Sorptive Uptake		
D_{app}/a^2 (s^{-1})[b]	1.1×10^{-7}	8.9×10^{-9}
K_d (L/kg)[c]	0.3	0.6
D_{app} (cm²/s)	7.0×10^{-11}	1.0×10^{-10}
τ_f[d]	7177	1309

[a] S, based on geometric mean (*1*); B, based on median of grain size distribution. [b] Best-fit values using eq 2 (see Figure 2). [c] Equilibrium K_d in batch experiment (Figure 2). [d] Tortuosity factor calculated based on eq. 5 and the bulk diffusion coefficient of TCE in water of 8.4×10^{-6} cm²/s at 20 °C (*17*).

The solid density of B, determined by water pycnometry, was 2.70 g/cm³. The grain size distribution of B was determined by combined wet sieving and sedimentation using the Casagrande method. Silt and clay contents were <8% and 2%, respectively. Three pulverized subsamples of B were analyzed for organic carbon by Desert Analytics (Tucson, AZ). The organic content (and relative standard deviation) was 0.15% (±0.013%).

Petrographic thin sections of B and S (two each) were prepared by Quality Thin Sections, Tucson, AZ, and analyzed for minerals based on physical appearance and optical properties. B and S are heterogeneous mixtures of minerals and lithic fragments, e.g., sedimentary rock fragments constitute 54% and 61% of the solids, respectively (Table I). Single-mineral grains were found in greater abundance in B than in S, as expected. N_2 adsorption/desorption (*21*, *22*) was used to determine specific areas and the intraparticle porosities (ϵ_i) in the 1.5–20-nm pore size range of the solids (Table I). The water contents (w) were determined by oven-drying at 110 °C to constant weight. The pore volumes in the column were calculated from the mass of solids added, the solids density, the water content, and the column volume.

Batch Sorption Experiments. The rate and equilibrium of TCE sorption under saturated conditions were studied in batch experiments using flame-sealed glass ampules according to procedures described previously (*2–4*, *23*). Briefly, ampules were filled with 50.0–60.0 g of solid, autoclaved for 20 min at 120 °C on three subsequent days, filled to the 60-mL mark with filter-sterilized (0.2 μm) groundwater from the field site, spiked by injecting neat TCE or a methanol solution of TCE, and flame-sealed immediately after spiking. After a thorough shaking, the ampules were stored in the dark at 20 ± 0.1 °C. Controls were filled with site groundwater. Samples

Table II. Column Properties, Conditions, and TCE Fraction Removed for Final Elution Runs in Each Set of Experiments

	B1	B3	S4	B2	B5
sample	bulk 100% RH	bulk wet	S wet	bulk dry	bulk dry
w (%)[a]	2.9	6.2	3.5	0.0	0.0
n (%)[b]	47.5	54.4	49.4	45.4	46.4
n_g (%)[c]	43.4	46.8	44.7	45.4	46.4
equilibration time (d)	5	5.8	23.2	3.0	5.5
$C_{0\ \text{breakthrough}}$ (mg/L)	68.3	27.3	75.7	17.6	
$C_{0\ \text{elution}}$[d] (mg/L)	46.4	14.7	27.6	10.0	14.9
flow rate (mL/min)	19.6	54.9	18.5	19.2	75.6
elution time (h)	22.6	71.3	105.6	662	490
$R_{0.5}$ elution[e]	1.7	1.5	1.1	475	345
end C/C_0	5.8×10^{-4}	1.6×10^{-4}	3.8×10^{-4}	3.4×10^{-3}	1.2×10^{-3}
$1-M_t/M_{0\ \text{end}}$[f]	0.70	0.54	0.43	0.98	0.95
$\text{TCE}_{\text{res. Conc.}}$ (mg/kg)[g]					
column inlet		14.8	29.8	6.8	14.1
column outlet		15.4	28.3	25.3	28.3

[a] w, water content based on dry mass of solids (m_d). [b] n, total porosity (air and water-filled porosity). [c] n_g, air-filled porosity. [d] Vapor-phase concentration after equilibration time. [e] Nondimensional retention volume at $C/C_0 = 0.5$. [f] Fraction of TCE removed from the column during the elution. [g] Residual TCE concentration in the solids measured by methanol extraction after the elution.

were periodically shaken by hand: several times during the first 48 h, every second day during the first week, once a week during the following month, and then twice a month (*4*) until analysis at 18 h, 2 d, 5 d, 11 d, and 84 d. Prior to sampling, ampules were mixed and centrifuged for 20 min at 230*g* and 20 °C. A total of 2 mL of supernatant water from the ampule was added to 2 mL of octane in PTFE-sealed hypovials (4 mL) and shaken for 30 min.

Column Experiments. HPLC columns (49.9-cm long, 2.11-cm i.d., Alltech) were packed with aquifer material and connected to a flame-ionization detector (FID, Hewlett-Packard) to measure on-line breakthrough and elution curves of TCE (*23*, *24*). All parts in contact with the volatiles (fittings, tubing, columns) were of stainless steel (ss), brass, or glass, except the valve seals which consisted of Teflon. A two position, six-port switching valve (Carle, Alltech) was used to direct the carrier gas (compressed air purified using an activated carbon filter) either through the column or through a bypass loop to the FID. To regulate the carrier gas flow, fine metering needle valves (brass) and brass toggle valves were used. The water content in the column was kept constant by passing the carrier gas through a 250-mL gas washing bottle filled with milli-Q water.

The TCE concentration in the carrier gas (C_0) was adjusted by changing the split ratio with two needle valves controlling the air flow to the TCE container and the column. Calibration of the FID was performed by sampling the carrier gas leaving the column with a gas-tight syringe (0.25 mL Series A-2, Dynatech Precision Sampling Corp., Baton Rouge, LA) and subsequent GC analysis of the sample. The FID response was linear in the concentration range used.

The linear velocities chosen in the column experiments were in the range of (1×10^{-3})–(8×10^{-3}) m/s, approximately the same order of magnitude as those observed in soil-air venting (as estimated from pressure gradients and air permeabilities given in refs 25 and 26). The porosities (47.5–54.5%) in the column packings were in the upper range or above the estimated porosity of this material in its natural setting, which range from 30% to over 55% (*27*).

Five different columns were studied (Table II): two wet and two dry B columns and one wet S column. Initially air-dried (at approximately 22 °C and 70% RH) B material

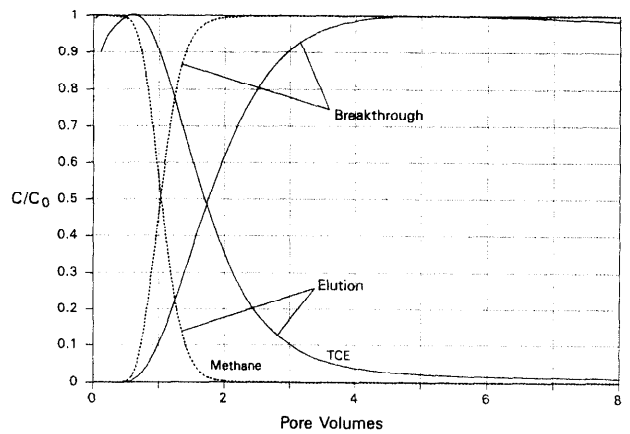

Figure 1. TCE and tracer (methane) breakthrough and elution curves in column B1 packed with bulk material at 100% RH ($w = 2.9\%$). C_0, input concentration in breakthrough experiments and initial concentration in elution experiments; C, column outlet concentration measured online by FID.

was equilibrated with carrier gas at 100% RH until weight constancy, which took 2 weeks. The average water content after 4 months was 2.9% and was invariant along the column length. B3 and S4 column weights were checked regularly and observed to be constant. In B3, water was added to adjust the water content to 6.2%. In B2 and B5, the columns were packed with oven-dried B material. In S4, the water content was adjusted to 3.5%.

The columns were characterized using methane (5% in argon) as the tracer gas. The system dead volume was 1.7 mL, 1% of the total column volume and less than 2% of the pore volumes (76.7–82.7 mL). No TCE sorption by the system components (column, tubes) and no leaks (at 40 psi) could be detected. Typical breakthrough and elution curves of methane and TCE in the column packed with aquifer material are shown in Figure 1.

After completion of the desorption experiments, the residual TCE concentration in the column was determined by equally dividing the solids into an inlet and an outlet sample. The samples were placed in 50-mL serum vials and immersed in methanol. The samples were periodically shaken by hand and stored at ambient temperature in the dark, and the supernatant methanol was analyzed repeatedly to assure equilibrium conditions. A constant concentration was reached after approximately 10 days.

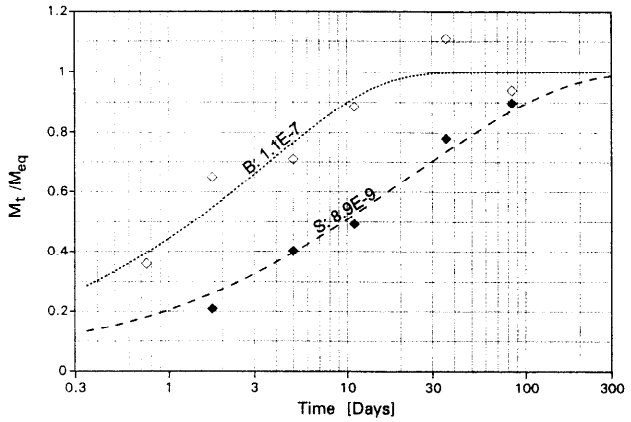

Figure 2. Fractional approach to equilibrium (M_t/M_{eq}) vs time in long-term aqueous batch experiments: data (symbols) and model fits (lines, eq 2); numbers on lines indicate D_{app}/a^2 (s^{-1}).

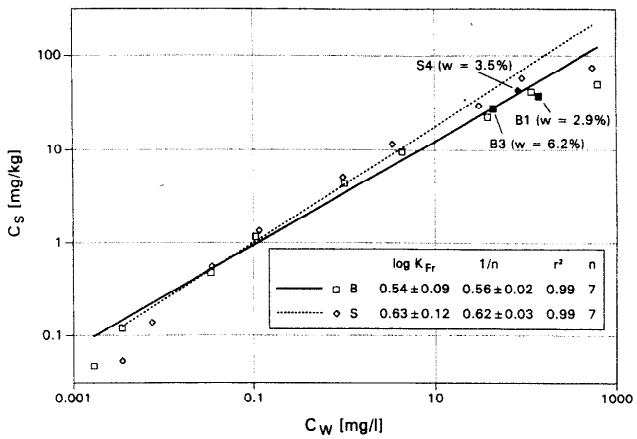

Figure 3. Sorption isotherms and Freundlich coefficients (linear regression of log data, highest and lowest concentration levels excluded) for bulk and S samples; filled symbols represent data from column experiments (Table II); w denotes water content.

Table II summarizes results and conditions of the column experiments. The reported experiments were conducted after several preliminary breakthrough and elution experiments. Mass balances were evaluated by integrating elution and breakthrough curves and the mass of TCE sorbed. Initial equilibration was achieved by passing TCE through the column to breakthrough, capping the columns at both ends, and equilibrating for days to weeks. During the equilibration (shut-in period), the pore gas concentrations (C_0) in the columns decreased (Table II) indicating continuing sorptive uptake of TCE.

Results and Discussion

Batch Studies. Apparent K_d values of S and B were measured in long-term experiments over a period of 84 days. The best fit for D_{app}/a^2 was obtained using the first 20 terms of eq 2 and minimizing the sum of the squared errors (Figure 2, Table I). The equilibrium K_d in B was reached after approximately 30 days. In S, a best fit to the model was achieved by assuming that 90% of the equilibrium K_d was reached in 84 d. The τ_f values given in Table I were calculated based on K_d, ϵ_i, and ρ_g (eq 5). The values obtained were of similar magnitude as those reported by Ball and Roberts (*3*) in batch studies (Borden sand). They were more than 2 orders of magnitude higher however than τ_f values predicted using the correlation $\tau_f = 1/\epsilon_i$, which was derived from steady-state diffusion experiments (*28*, *29*) and which is analogous to Archie's law (*30*). This disagreement points toward significant discrepancies between assumed and real properties of the solids. The assumptions that the aquifer material was homogeneous appears especially tenuous. Weber et al. (*31*) report that shale-like materials in soil samples showed sorption capacities approximately 100 times higher than the parent bulk material. In the Santa Clara material studied here, shale fragments constitute 13–19% of the bulk (Table I). Assuming that sorption preferentially takes place in the shale fraction would result in a grain specific K_d almost 2 orders of magnitude larger than the bulk K_d and in an equivalent decrease of the tortuosity factors (eq 5) which is relatively close to the values predicted based on the empirical correlations (*28–30*). The higher tortuosity factor obtained for B as compared to S may be due to uncertainities in estimating the nominal particle radius for B as the characteristic length scale for diffusion. The geometric mean which was used as the nominal radius for S represents a uniform size only if the size distribution is confined to a narrow range (*1*). For B where only about 80% of the particle size ranged within 1 order of magnitude (0.2–2 mm), the nominal radius was estimated based on the median of the grain size distribution. If in B the larger size fraction was responsible for most of the sorption, a larger nominal radius would apply, which reduces τ_f significantly (e.g., 2-fold increase in the nominal radius results in 4 times lower τ_f).

The sorption isotherms measured for the saturated B and S samples after 84 days of equilibration were consistent with the Freundlich model (Figure 3) except for the highest and lowest concentration levels (which were excluded from the linear regression of the log–log data). The two isotherms were very similar in spite of the higher silt/clay content of B. Perhaps the majority of the sorption sites were associated with the relatively coarse rock fragments, as suggested previously (*2*, *8*), rather than with the silt- and clay-sized single-mineral grains. The isotherms in Figure 3 also include data from the unsaturated columns packed with wet B and S material. K_d values obtained in the batch and the unsaturated column system (eq 1) agreed, indicating that Henry's law is applicable to calculate pore water concentrations, as reported previously (*10*, *12*).

Column Studies: Breakthrough and Elution Behavior in Moist Samples (B1, B3, S4). For methane, the breakthrough and elution curves in moist columns were sigmoidal and highly symmetrical (Figure 1) and consistent with conservative behavior (nondimensional retention volumes obtained at $C/C_0 = 0.5$ were $1.03 \pm 3.4\%$, $n = 10$). The breakthrough volumes of subsequent column packings agreed within 3.6% with the gravimetrically determined pore volumes, indicating uniform flow conditions. The mass of TCE retained by a column or removed from a column was obtained by integrating the areas above and below the breakthrough and elution curves, respectively (*23*). For TCE, the breakthrough occured after approximately 4.5 pore volumes, see Figure 1. For TCE, the nondimensional retention volumes, $R_{0.5}$, were below 2 and much lower than expected, based on the equilibrium K_d values from the batch experiments, indicating that equilibrium was not reached. In the elution experiment, C/C_0 decreased to below 5% after 4 pore volumes and after that decreased only very slowly.

The effect of equilibration time, initial equilibrium concentration, and water content on desorption behavior

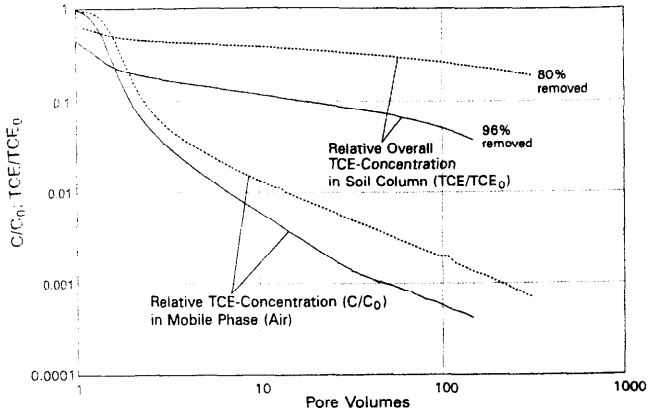

Figure 4. Relative concentrations in the carrier gas (C/C_0), compared to the decrease of the overall normalized TCE content in the column (TCE/TCE_0) after equilibration for 23 min (solid lines) and 6 d (dashed lines) in B3. Conditions for 23-min and 6-day equilibration, respectively: flow rates; 17.3 and 18.5 mL/min; vapor-phase concentrations, 40.9 and 43.3 mg/L; TCE mass at time zero: 6.1 and 10.6 mg.

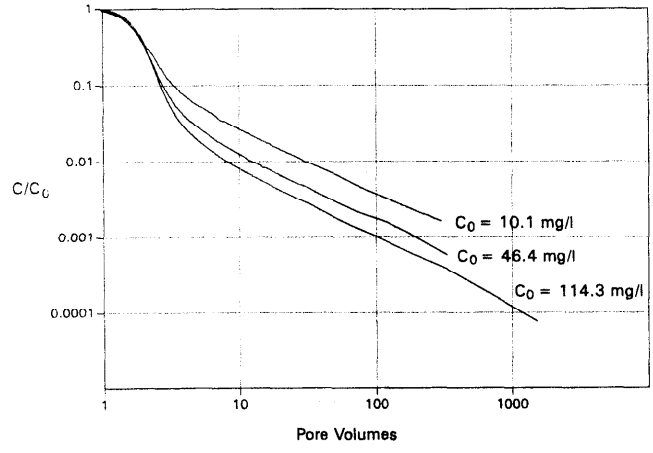

Figure 5. Effect of initial concentration on the elution profile in B1; flow rates were approximately 19 mL/min.

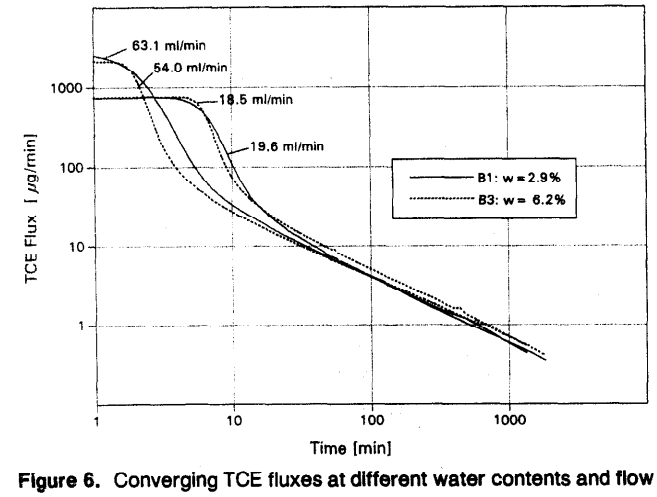

Figure 6. Converging TCE fluxes at different water contents and flow rates in the wet columns.

was investigated in a series of desorption experiments shown in Figures 4–6. The desorption experiments were conducted over a time scale of a few days, and only 30–50% of the mass sorbed was removed. Short-term (1–2 days) experiments, therefore, only reflect the desorption behavior of a fraction of the total mass adsorbed. When the equilibration period was short (23 min), 96% of the mass (in column B1) was removed after 100 pore volumes (Figure 4). Presumably, during short exposure, TCE fully

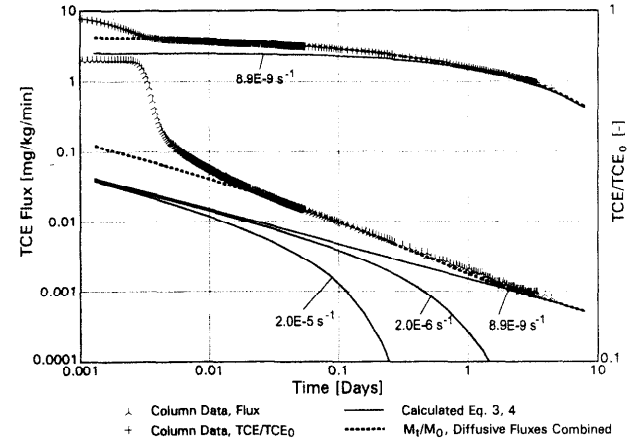

Figure 7. TCE flux and overall normalized TCE content in the column (TCE/TCE_0) vs time for the S sample: comparison between column elution data (symbols) and model results using eqs 3 and 4 (lines). The dashed lines represent TCE/TCE_0 and q assuming a fast- ($D_{app}/a^2 = 2 \times 10^{-5}$), medium- ($D_{app}/a^2 = 2 \times 10^{-6}$), and slow-desorbing fraction ($D_{app}/a^2 = 8.9 \times 10^{-9}\ s^{-1}$, from long-term batch experiment) combined.

penetrated only the readily accessible sites whereas only 4% reached slow sites. When equilibration was longer than 5 days, 73% or less of the mass of TCE was removed after 100 pore volumes (8 h). Because there was no significant difference between the 6-d and 24-d elution profile, equilibration times in the range of 4–6 d were used for the subsequent experiments. For the larger S fraction, elution profiles remained unchanged after 10 d of equilibration. Similar findings were reported by Pignatello (*33*).

The decline of C/C_0 was faster when C_0 was higher (Figure 5). This may be explained by the nonlinearity of the sorption isotherms (Figure 3) which result in a relative increase of TCE sorption and thus decreasing D_{app} with decreasing C_0. The desorption rates measured in B1 and B3, obtained at similar C_0 but different flow rates and different water contents, converged after less than 20 min or about 30–40 pore volumes (Figure 6). The fact that the TCE desorption rates were independent of flow rate and water content indicates that mass transfer limitations are occurring in the intraparticle or intrasorbent domain rather than in the intergranular water.

In all cases, C/C_0 decreased rapidly to less than 1% when a few pore volumes were displaced. This initial purge removed the vapor-phase fraction of about 15–30% of the total TCE content of the column. Thereafter, the TCE fluxes (indicated in µg/min or normalized as C/C_0) decreased only slowly with relatively constant negative slopes on log–log plots. The slopes were approximately −0.8, steeper than the value predicted by the model for short desorption times (−0.5), indicating that resistance to desorption increases faster with decreasing solids concentration than predicted by the model. Model calculations based on eqs 3 and 4 are compared in Figure 7 using data obtained with S4. A nearly perfect fit could be achieved by assuming a slow-, medium-, and fast-desorbing grain population, each contributing to the total flux. The slow-desorbing population was modeled based entirely on the D_{app}/a^2 determined in the long-term batch sorption experiments (Table I, Figure 2) and agreed very well with the diffusive fluxes measured after 2 days. In order to fit the early time data, two fast-desorbing grain populations were used with a D_{app}/a^2 of 2×10^{-5} and $2 \times$

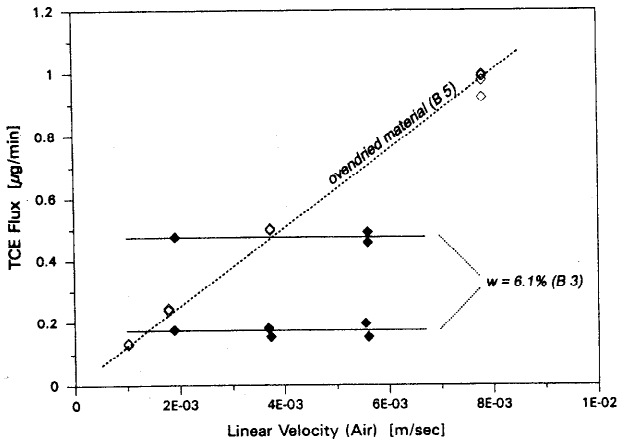

Figure 8. Influence of linear velocity on TCE fluxes in wet (B3) and dry (B5) columns (mobile phase concentration: $C/C_0 < 3 \times 10^{-3}$, Table II). Desorption in B5 was measured after 20 d, in B3 after 1 d (upper) and 3 d (lower) of continuous elution.

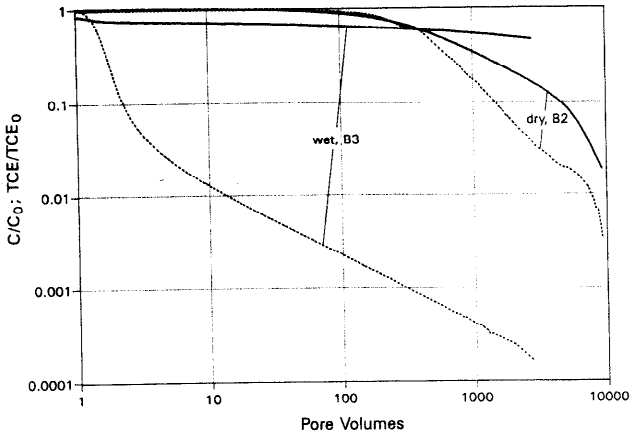

Figure 9. Comparison of C/C_0, the normalized effluent TCE concentration (dashed lines), and TCE/TCE_0, the overall normalized TCE content (solid lines), in wet and dry columns as a function of pore volumes displaced.

10^{-6} s^{-1}, which accounted for 2% and 5.9% of the total sorption capacity of the solids.

Desorption from Dry Samples. In the dry columns B2 and B5, the mass retained in the columns was measured at linear velocities of 2.0×10^{-3} and 7.8×10^{-3} m/s (flow rates of 19.2 and 75.6 mL/min, respectively). In contrast to the wet columns, methane was slightly retarded ($R_{0.5}$ = 1.25), presumably due to adsorption on mineral surfaces with no or only thin water films. Sorption of TCE in the dry columns, as indicated by the nondimensional retention volumes at $C/C_0 = 0.5$, was much stronger ($R_{0.5}$: 475 and 345 for B2 and B5, respectively; Table II) than in the wet columns which was to be expected from previous investigations (*10*, *11*). As is evident from the data shown in Figure 8, the long-term TCE desorption rate from the dry columns increased proportionally with the gas velocity, in contrast to the wet columns where it was independent of flow rate. These desorption rates were measured after extended desorption at low C/C_0 ($<3 \times 10^{-3}$) for B2 and B5 which had similar initial as well as similar residual concentrations (methanol extraction, Table II). In the dry material, intraparticle mass transfer was not limited or only to a lesser extent. After eluting B2 and B5 for 662 and 490 h, respectively, TCE removal was nearly complete, with only 2 and 5% remaining (Table II). The rapid removal of TCE from the dry B2 column as compared to the slow removal from the wet B3 column is also evident from data shown as compared to the slow removal from the wet B3 column is also evident from data shown in Figure 9. In the dry columns, the time profile of the flux closely corresponded to the residual TCE content, consistent with near-equilibrium conditions. In contrast, in the wet columns the flux decreased rapidly to insignificant levels, although the residual TCE content (TCE/TCE_0) remained high. At the end of the dry column experiments, the TCE concentration in the solids was lower at the column inlet, where C/C_0 was zero, than at the column outlet (methanol extraction, Table II), whereas no concentration gradient in the wet columns was observed.

The fact that desorption was faster in the dry solids compared to the wet solids, in spite of the greater sorption capacity, suggests that mass transfer was due to vapor phase diffusion, unhindered by water or organic matter. Diffusion coefficients in vapor phase are about 4 orders of magnitude larger than in water (*17*).

Summary and Conclusions

Sorptive uptake of TCE was measured in a batch system under saturated conditions using Santa Clara aquifer material and compared to sorption and desorption in soil chromatographic columns under unsaturated conditions at close to 100% RH. The K_d values measured in the water–solid system agreed well with the pore water–solid K_d values, determined in the unsaturated system using the measured gas-phase concentration and Henry's law constant to determine the pore water concentration (eq 1). This agreement indicates that (i) water present in the moist soils (RH > 95%) has the same properties as bulk water and (ii) K_d values determined in batch studies can be used in conjunction with reported Henry's coefficients for calculating the solid–air partition coefficients in wet but unsaturated material.

The tortuosity factors calculated from the diffusion rate constants, determined in the long-term batch experiment, agreed well with literature values obtained in batch studies but disagreed with those obtained under steady-state conditions (*28–30*). This disagreement points toward significant discrepancies between assumed and real properties of heterogeneous materials and a need to characterize the sorption properties of individual components.

The chromatographic technique employed here proved especially practical to study the desorption of the contaminants from aquifer materials. After the wet columns were purged with 2–10 pore volumes, the TCE concentration in the vapour phase dropped to less than 2% of the initial concentration. Thereafter, the rate of compound removal was independent of the linear velocity of the carrier gas, indicating intraparticle mass transport limitations occur inside the wet particles. Removal of water from micro- and mesopores by oven drying at 110 °C significantly increased the rate of desorption in spite of the fact that the sorption capacity of the dry solids increased about 400 times. In dry columns, after 20 days of venting, the TCE flux still increased proportionally with the linear velocity of the carrier gas within the range of (2.0×10^{-3})–(7.8×10^{-3}) m/s, indicating that a much larger fraction of the sorbed TCE was in rapid equilibrium with the gaseous phase. The fact that removal of water from the Santa Clara aquifer material significantly increased the TCE desorption rate was taken as an indication that slow diffusion in water-filled pores may limit intraparticle mass transfer, as suggested by Ball and Roberts (*2*, *3*).

Removal of TCE by soil venting from the wet material was modeled using the intraparticle diffusion model. When the model was calibrated using only the D_{app}/a^2 determined in the long-term batch experiments, it agreed well with the data observed for the venting period after 1 day (Figure 7). The TCE flux measured earlier could be fitted assuming two fast-desorbing fractions accounting for 7.9% of the total sorption capacity of the solids. The diffusion model predicts for short periods of time ($t < 0.01a^2/D_{app}$) a TCE flux decreasing at a constant slope of −0.5 on a log–log plot and for long periods of time ($t > 0.1a^2/D_{app}$) a desorption rate which follows a first-order process. When D_{app}/a^2 and M_0 are known, the time necessary to remove a certain fraction of the contaminant and the corresponding fluxes may be estimated (eqs 3 and 4). The results agree with the proposition that soil-air venting and pump-and-treat systems are typically operated far from equilibrium due to slow desorption from solids. The frequently observed rapid initial removal rates are likely due to advective–dispersive removal of contaminants existing in the mobile phase (groundwater, air) and rapidly desorbing from the soil solids or dissolving from nonaqueous phases. Removal of the residual fraction occurs on time scales that are orders of magnitude larger. The observed slow desorption rates have wide reaching implications and need to be further evaluated, both from an engineering and a regulatory point of view.

Acknowledgments

This work was supported in part by the U.S. EPA Office of Exploratory Research, Washington, DC through Grant R-812913, by Schlumberger Technologies through the U.S. EPA-supported Western Region Hazardous Substance Research Center, by the Deutsche Forschungsgemeinschaft through a scholarship to P.G., by PWAB, Baden-Würtemberg, Germany, and by the Eidgenössische Technische Hochschule, Zürich, through a visiting professorship to M.R. The content of this paper does not necessarily represent the view of these organizations. We appreciate valuable discussions with W.P. Ball (The Johns Hopkins University), James Farrell, and Charles Werth (Stanford University).

Literature Cited

(1) Wu, S.-C.; Gschwend, P. M. *Environ. Sci. Technol.* **1986**, *29*, 717–725.
(2) Ball, W. P.; Roberts, P. V. *Environ. Sci. Technol.* **1990**, *25*, 1223–1237.
(3) Ball, W. P.; Roberts, P. V. *Environ. Sci. Technol.* **1990**, *25*, 1237–1249.
(4) Ball, W. P. Ph.D. Dissertation, Standford University, 1989.
(5) Pignatello, J. J.; Frink, C. R.; Marin, P. A.; Droste, E. X. *J. Contam. Hydrol.* **1990**, *5*, 195–214.
(6) Karickhoff, S. W.; Morris, K. S. *Environ. Toxicol. Chem.* **1985**, *4*, 469–479.
(7) Brusseau, M. L.; Jessup, R. E.; Rao, P. S. *Environ. Sci. Technol.* **1991**, *25*, 134–143.
(8) Harmon, T. Ph.D. Dissertation, Stanford University, 1992.
(9) Farrell, J. Ph.D. Dissertation, Stanford University, 1992.
(10) Grathwohl, P. *Tübinger Geowissensch. Arbeiten* **1989**, *1*, 1–102.
(11) Chiou, C. T.; Shoup, T. D. *Environ. Sci. Technol.* **1985**, *19*, 1196–1200.
(12) Dorris, G. M.; Gray, D. G. *J. Phys. Chem.* **1981**, *85*, 3628–3635.
(13) Kinniburgh, D. G. *Environ. Sci. Technol.* **1986**, *20*, 895–904.
(14) Crank, J. *The Mathematics of Diffusion*, 2nd ed.; Oxford University Press: Oxford, 1975.
(15) Häfner, F.; Sames, D.; Voigt, H.-D. *Heat and Mass Transfer*; Springer Verlag: Berlin, 1992; p 626.
(16) Grathwohl, P.; Gewald, T.; Pyka, W.; Schüth, C. *Contaminated Soil 93*; Arendt, F., Annokkée, Bosman, R., van den Brink, W. J., Eds.; Kluwer: Dordrecht, The Netherlands; 1993; pp 175–184.
(17) Lyman, W. J.; Reehl, W. F.; Rosenblatt, D. H. *Handbook of Chemical Property Estimation Methods*; ACS: Washington, DC, 1990.
(18) Gossett, J. M. *Environ. Sci. Technol.* **1987**, *21*, 202–208.
(19) Page, B. M. In *Geology of Northern California*; Bailey, E. H., Ed., California Division of Mines and Geology: San Francisco, 1966.
(20) Meade, R. H. *U.S. Geol. Surv. Prof. Pap.* **1967**, *No. 497-C*.
(21) Brunauer, S.; Emmet, P. H.; Teller, E. *J. Am. Chem. Soc.* **1938**, *60*, 309–319.
(22) Gregg, S. J.; Sing, K. S. W. *Adsorption, Surface Area and Porosity*; Academic Press: New York, 1982.
(23) Grathwohl, P.; Reinhard, M. Sorption and Desorption Kinetics of Trichloroethylene in Aquifer Material under Saturated and Unsaturated Conditions. Western Region Hazardous Substance Research Center, Technical Report No. 2, Stanford University, Stanford, CA, 1991.
(24) Farrell, J.; Reinhard, M. Measurement of Organic Vapor Isotherms on Wet Soils and Aquifer Materials. In *Current Practices in Ground Water and Vadose Zone Investigations*; Nielsen, D. M., Sara, M. N., Eds.; ASTM STP 1118; American Society for Testing Materials: Philadelphia, 1991.
(25) Croise, J.; Kinzelbach, W.; Schmolke, J. *Proceedings of the IAHR-Symposium Contaminant Transport in Groundwater*, Stuttgart, Germany, 1989; Balkema: Rotterdam, The Netherlands, 1989; pp 437–444.
(26) Brauns, J.; Wehrle, K. *Schr. Angew. Geol. Karlsruhe* **1990**, *9*, 123–142.
(27) Johnson, A. I.; Moston, R. R.; Morris, D. A. *U.S. Geol. Surv. Prof. Pap.* **1968**, *No. 497-A*.
(28) Wakao, N.; Smith, J. M. *Chem. Eng. Sci.* **1962**, *17*, 825.
(29) Grathwohl, P. *Proceedings of the 7th International Symposium on Water-Rock Interactions*; Kharaka, Y. K., Maest, A. S., eds.; WRI-7: Park City, UT, 1992; pp 283–286.
(30) Archie, G. E. *Trans. Am. Inst. Min., Metall. Pet. Eng.* **1942**, *146*, 54–61.
(31) Weber, W. J.; McGinely, P. M.; Katz, L. E. *Environ. Sci. Technol.* **1992**, *26*, 1955–1962.
(32) Nkedi-Kizza, P.; Rao, P. S. C.; Hornsby, A. G. *Environ. Sci. Technol.* **1987**, *21*, 1107–1111.
(33) Pignatello, J. J. *Environ. Toxicol. Chem.* **1991**, *10*, 1399–1404.

Received for review November 30, 1992. Revised manuscript received July 12, 1993. Accepted July 22, 1993.[⊗]

[⊗] Abstract published in *Advance ACS Abstracts*, September 15, 1993.